WIKIPEDIA
The Free Encyclopedia

Google Scholar

In mathematics, physics, and art, moiré patterns are large-scale interference patterns… For the moiré interference pattern to appear, the two patterns must not be completely identical, but rather displaced, rotated, or have slightly different pitch.

Twistronics (from twist and electronics) is the study of how the angle (the twist) between layers of two-dimensional materials can change their electrical properties.

twistronics + moiré $\longrightarrow$ over 20,000 papers

Morning: Moiré superlattices in graphene	Afternoon: Twistronics of transition metal dichalcogenides

Graphene superlattices

- Moiré superlattice (SL) in heterostructures graphene/hexagonal boron nitride (G/hBN)
- Weak lattice relaxation in G/hBN
- Super-moiré structures
- Brown-Zak magnetic minibands ('Hofstadter butterfly') and 'kagome' oscillations
- Moiré SL effects in BLG and thin graphitic films

graphene

$$\hat{H} = v\vec{\sigma}\cdot\vec{p}$$

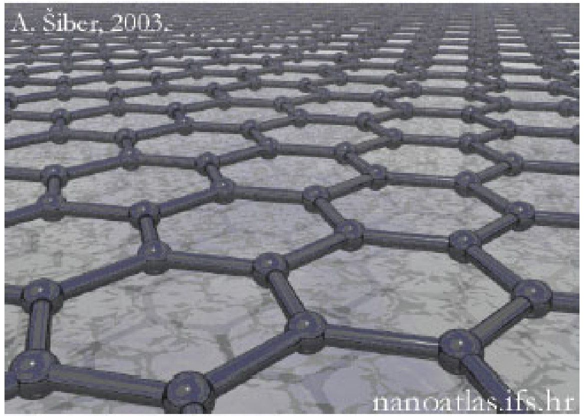

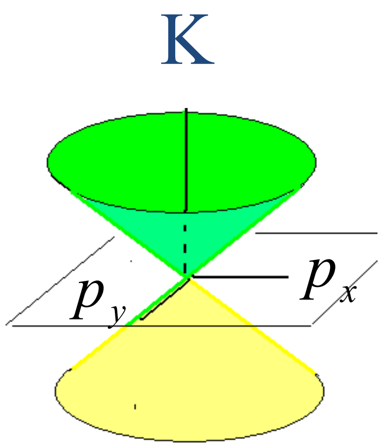

Graphene (monolayer of graphite) is an atomically thin (2D) zero-gap semiconductor with linear dispersion of conduction and valence band electrons.

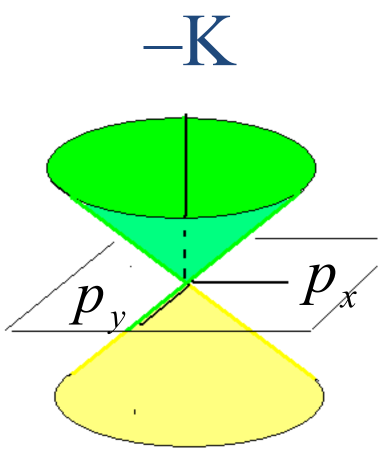

Graphene: gapless semiconductor with Dirac electrons

$$\hat{H} = v\vec{\sigma}\cdot\vec{p}$$

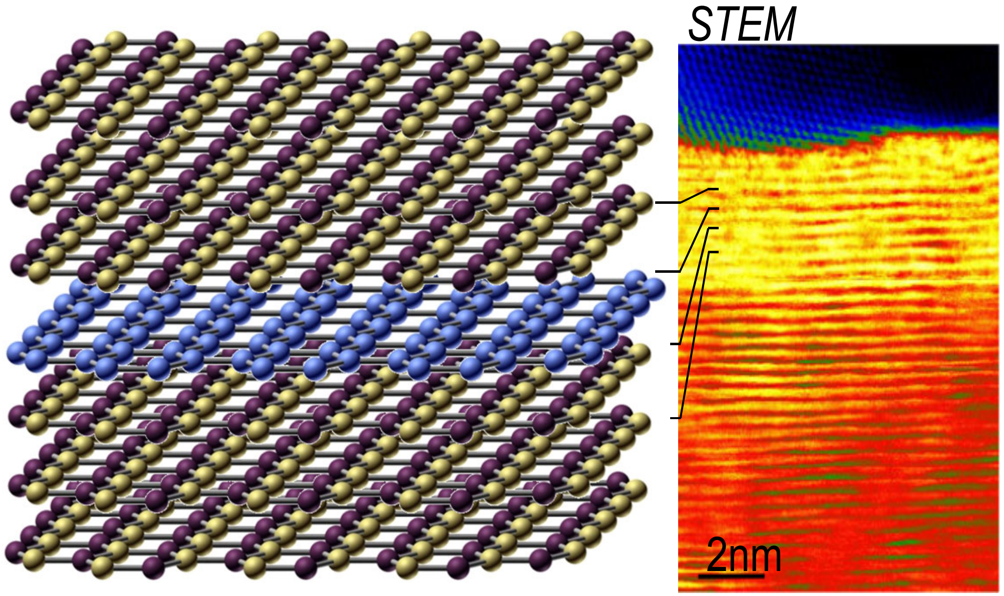

hBN ('white graphene') sp^2 – bonded insulator with a large band gap, Δ >5eV

$$\hat{H} = \Delta\sigma_z + v'\vec{\sigma}\cdot\vec{p}$$

both crystals have honeycomb lattices with a $\delta=0.018$ mismatch between lattice constants

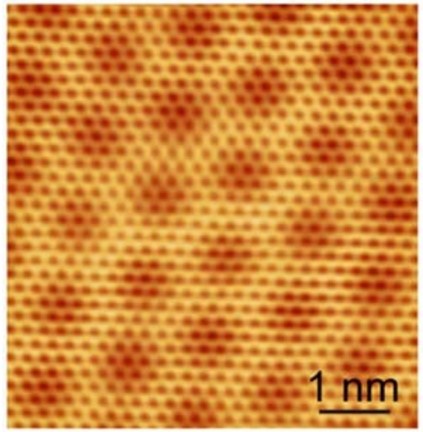

which produces moiré pattern

Xue, et al, Nature Mat 10, 282 (2011)

Long-period moiré patterns are generic for all G/hBN heterostructures, grown or mechanically transferred

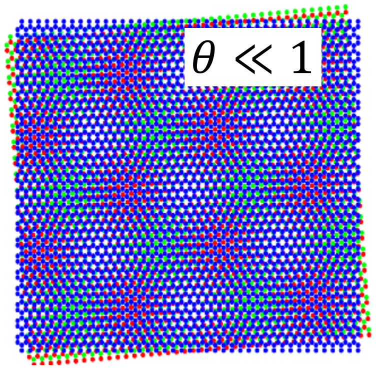

$$A \approx \frac{a}{\sqrt{\delta^2 + \theta^2}}$$

lattice mismatch (slightly different pitch)

rotated

Bloch states in one layer experience Bragg scattering from the lattice of the other layer (umklapp process)

For the interlayer distance longer than the lattice constant (or even comparable) the dominant – for the interlayer coupling – reciprocal space points belong to the first star, which determines the main star in the reciprocal space of moiré superlattice: $b = G_g - G_{hBN}$

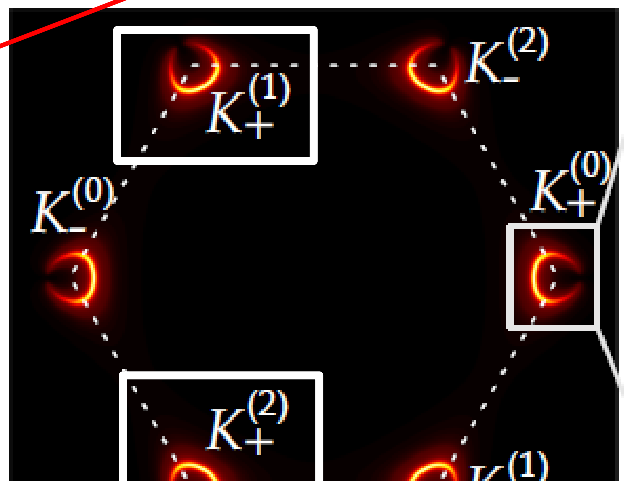

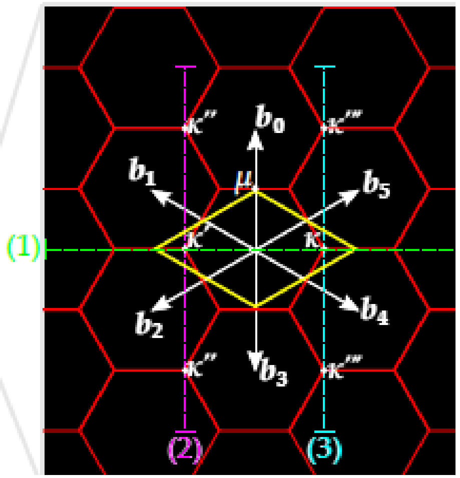

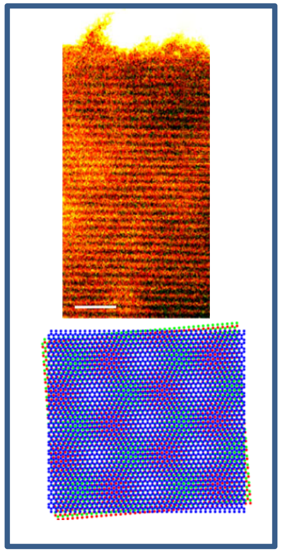

electrons in G/hBN moiré superlattices

Due to the longer distance between graphene and hBN layers than their lattice constants, moiré perturbation is dominated by simple *b*-harmonics.

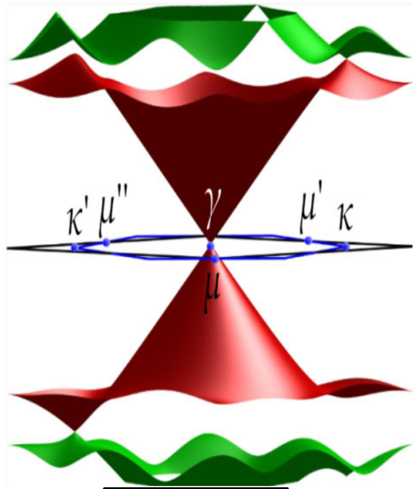

$$\kappa' = \sqrt{\delta^2 + \theta^2}\, K' << K'$$

electrostatic modulation

sublattice asymmetry

modulated hopping between sublattices (e.g., due to strain), leading to a 'pseudomagnetic' field

$$\hat{H} = vp\cdot\sigma + u_0 vbf_1(r) + u_3 vbf_2(r)\sigma_3\tau_3 + u_1 v\left[l_z \times \nabla f_2(r)\right]\cdot\sigma\tau_3$$

inversion symmetric

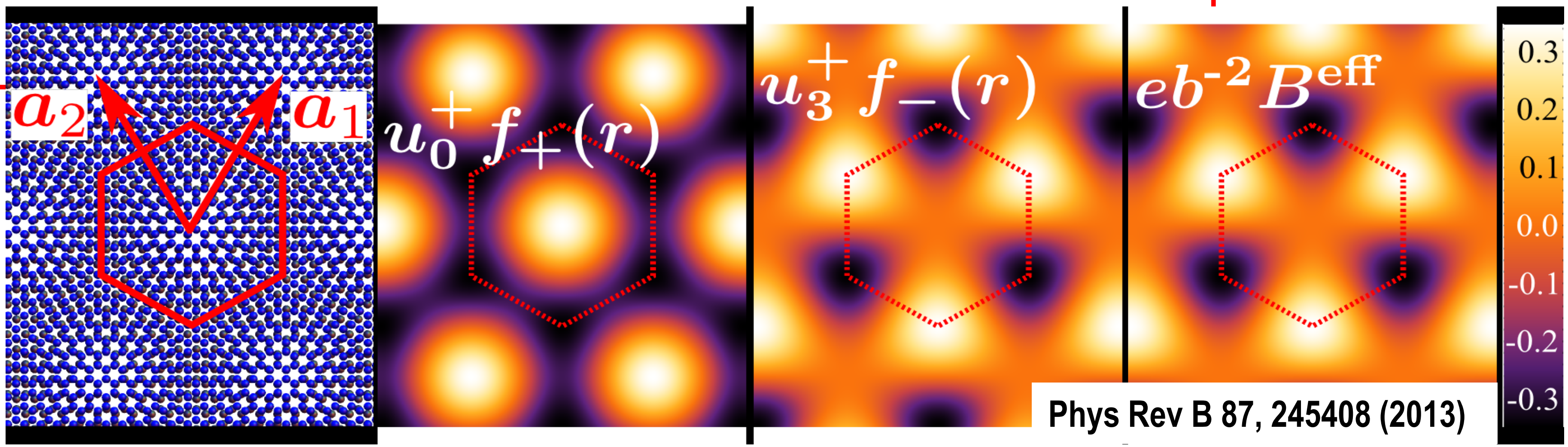

Umklapp e-e scattering in G/hBN moiré superlattices

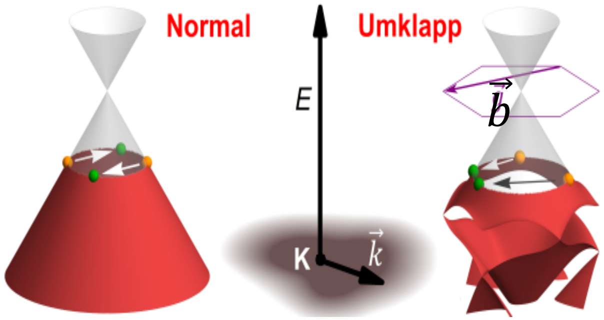

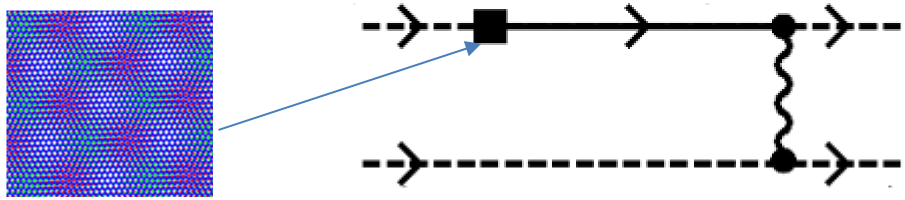

$$\vec{k}_1 + \vec{k}_2 = \vec{k}_3 + \vec{k}_4 + \vec{b}$$

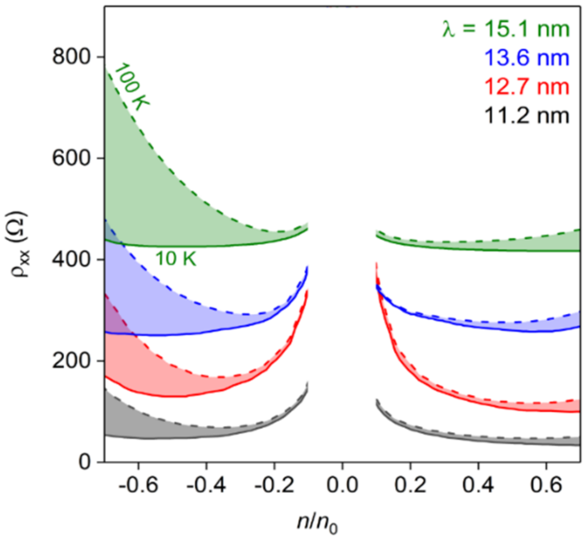

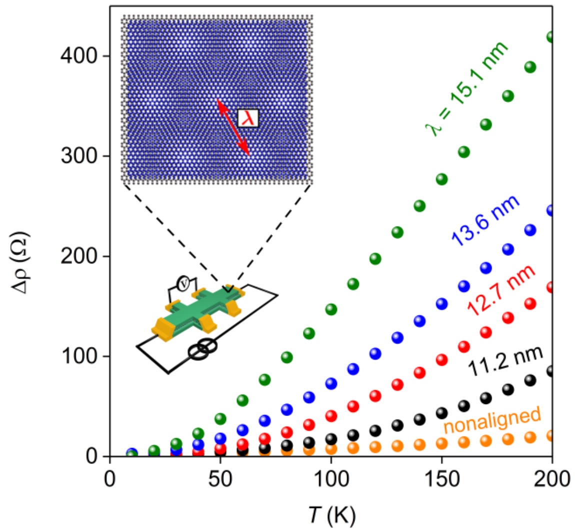

T=100K

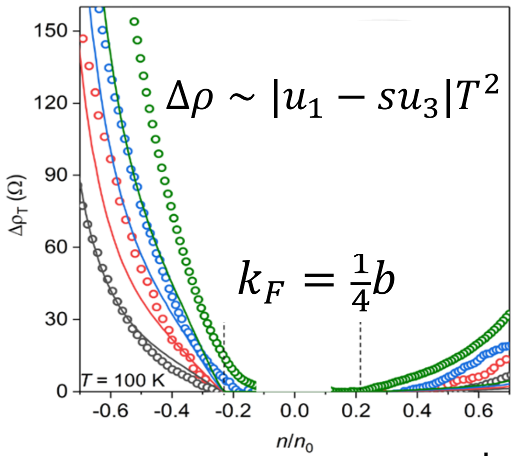

$s = -$ $\qquad$ $s = +$

Nature Physics 15, 32 (2019)

Umklapp e-e scattering in BLG/hBN moiré superlattices

$$\rho_{\mathrm{Uee}} \propto |n - n_*|^{1/2} |n|^{-2} T^2$$

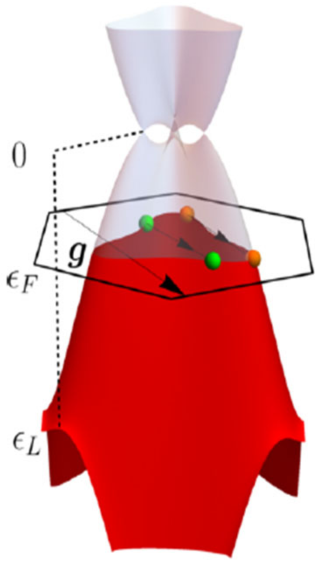

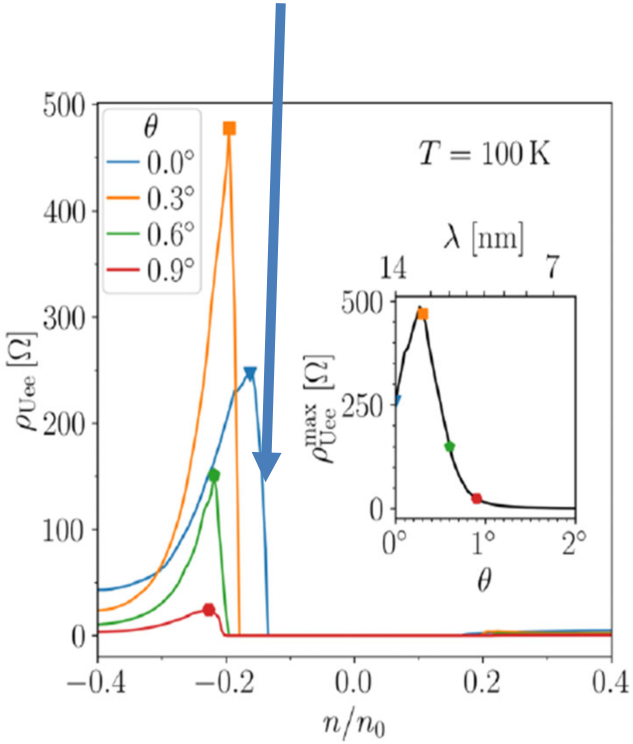

Phys Rev B 107, 144111 (2023)

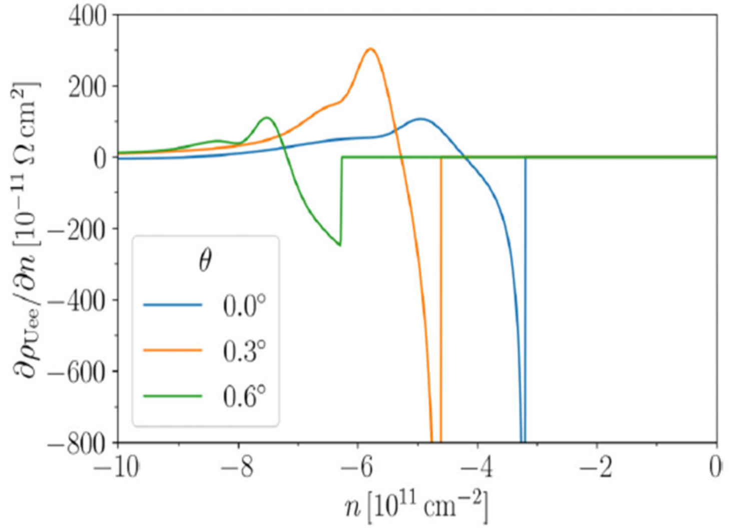

room-temperature transistor operation in metallic regime

Moiré minibands: manifestation in magneto-transport and capacitance spectroscopy

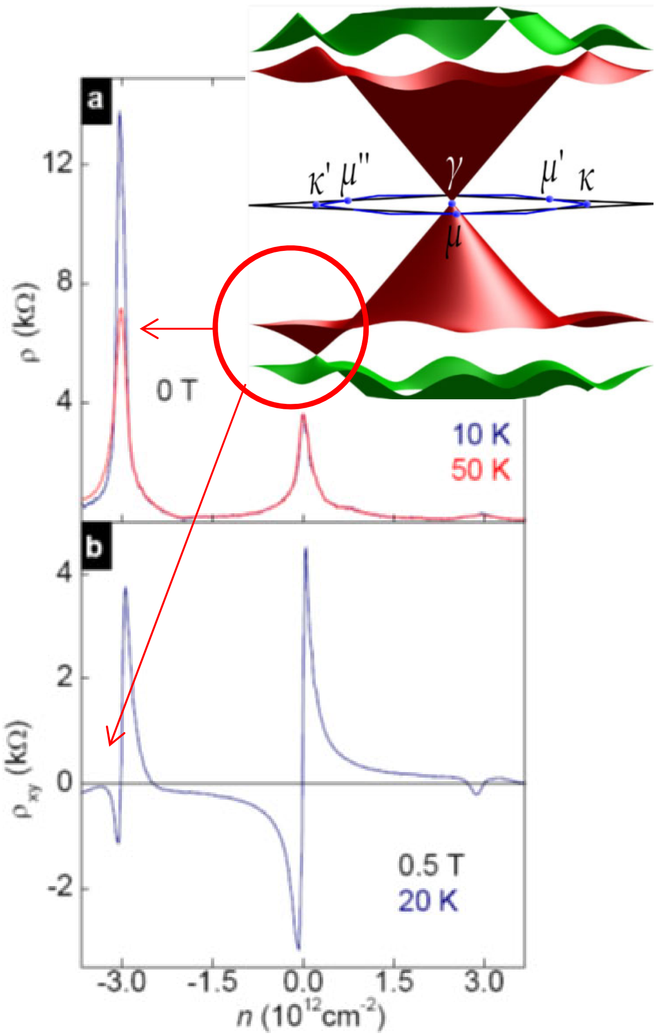

Nature 497, 594 (2013)

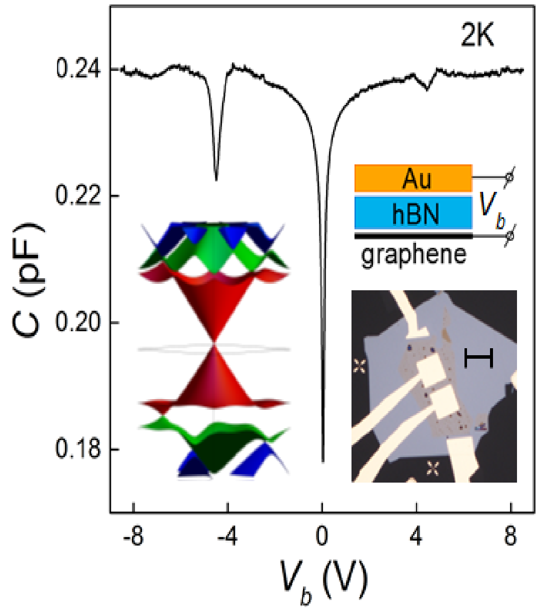

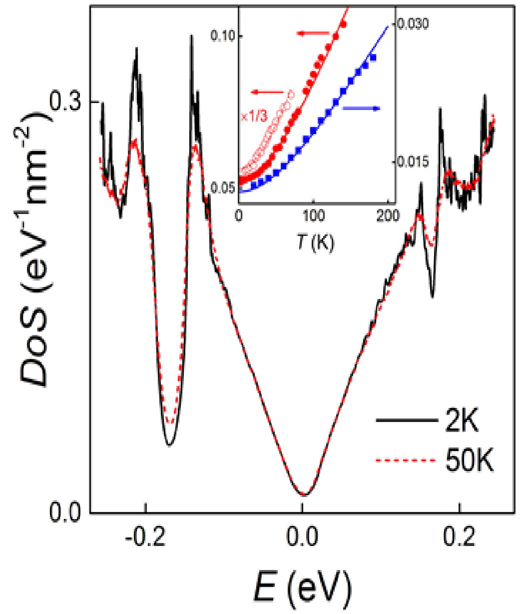

Nature Physics 10, 525 (2014)

Transverse magnetic focusing of ballistic electrons in moiré minibands in almost aligned G/hBN (low T)

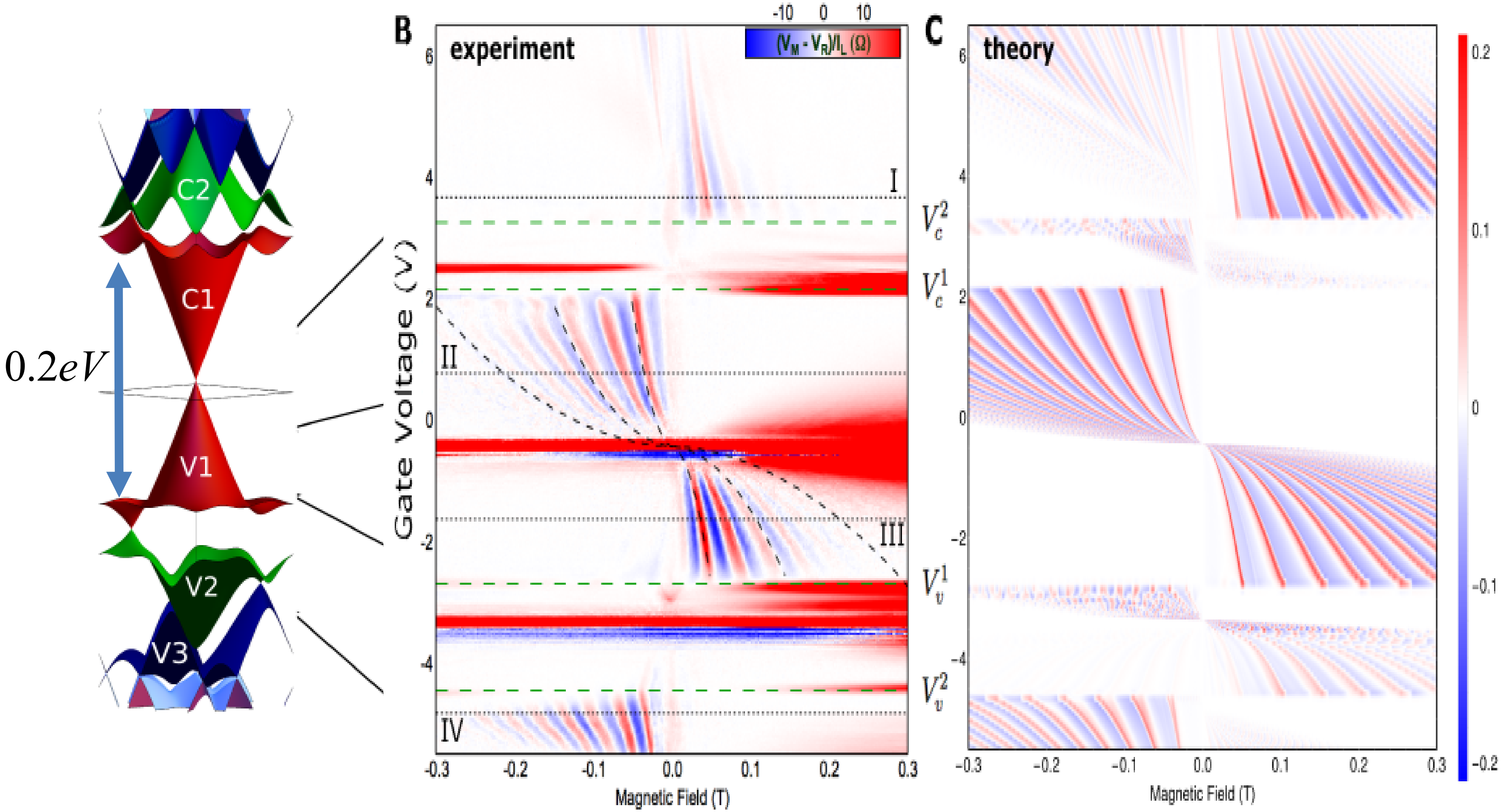

Science 353, 1526 (2016)

Landau levels of Dirac electrons in a magnetic field

$$H = v(\vec{p} - \tfrac{e}{c}\vec{A}) \cdot \vec{\sigma} \;\Rightarrow\; \varepsilon^{\pm} = \pm\sqrt{2n}\,\frac{v}{\lambda_B} \propto \sqrt{n \cdot B}$$

4-fold degenerate
Landau level

McClure - Phys. Rev. 104, 666 (1956)

the largest gaps in the LL spectrum

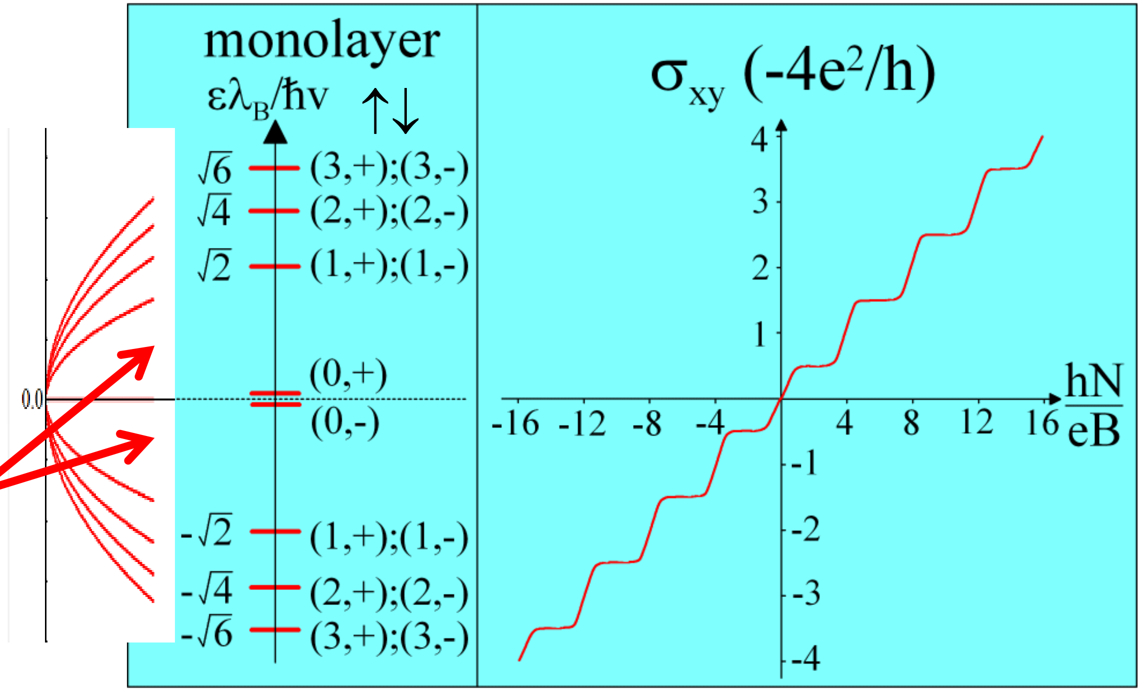

Should be the same for the secondary Dirac electrons at the edge of the 1st moiré miniband

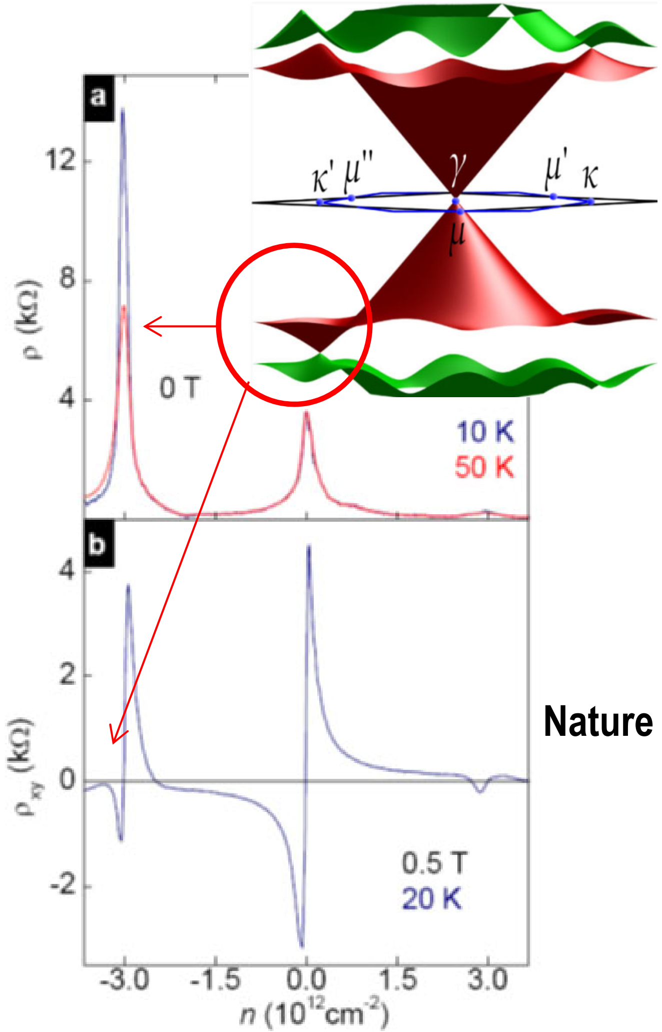

Magneto-transport in oriented graphene-BN heterostructures

Nature 497, 594 (2013)

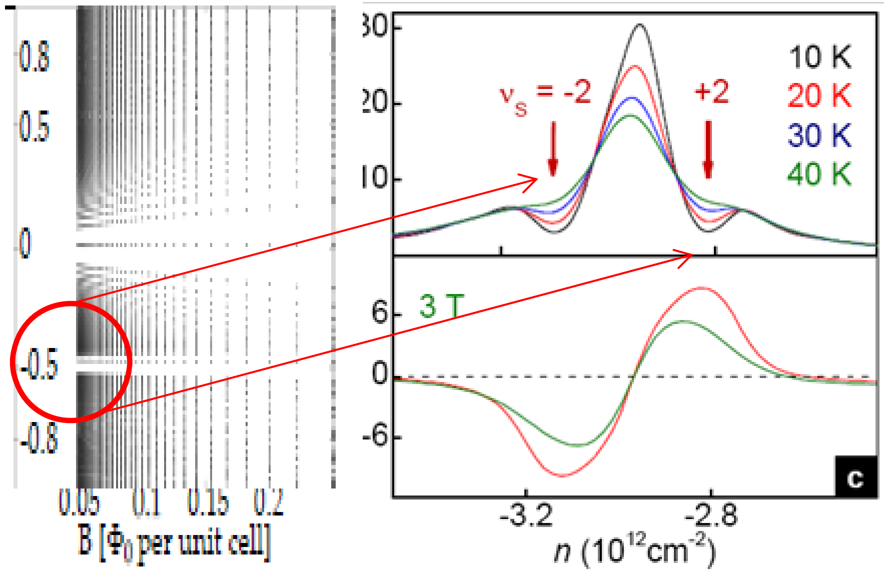

Magneto-capacitance

Nature Physics 10, 525 (2014)

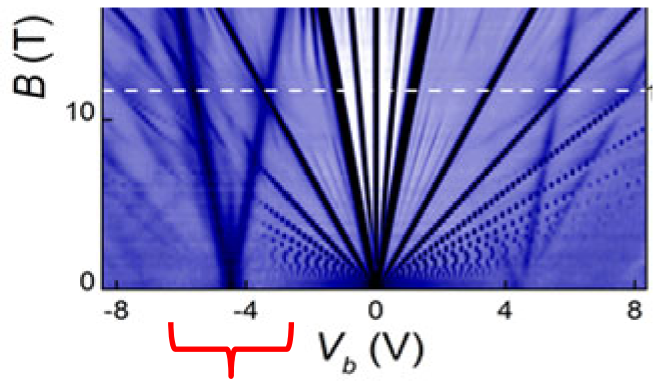

Graphene superlattices

- Moiré superlattice (SL) in heterostructures graphene/hexagonal boron nitride (G/hBN)
- Weak lattice relaxation in G/hBN
- Super-moiré super-structures
- Brown-Zak magnetic minibands ('Hofstadter butterfly') and 'kagome oscillations'
- Moiré SL effects in BLG and thin graphitic films

Strong *versus* weak lattice relaxation

$$\sum_{l=t,b}\left[(\lambda_l/2)\left(u_{ii}^{(l)}\right)^2+\mu_l\left(u_{ij}^{(l)}\right)^2\right]+W_{P/AP}(\boldsymbol{r}_0,d)$$

$$\boldsymbol{r}_0\left(\boldsymbol{r}\right)=\theta\hat{z}\times\boldsymbol{r}+\delta\boldsymbol{r}+\boldsymbol{u}^{(t)}-\boldsymbol{u}^{(b)}$$

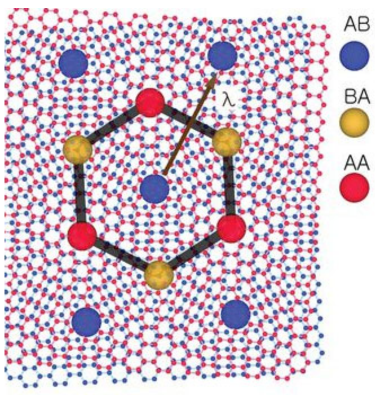

tBLG: for long-period moiré SL (small angles ≤1°) energy cost of shear strain at domain walls can be taken over by adhesion energy gain inside the Bernal-stacking domains: formation of domain patterns in marginally twisted bilayers (Koshino's lecture)

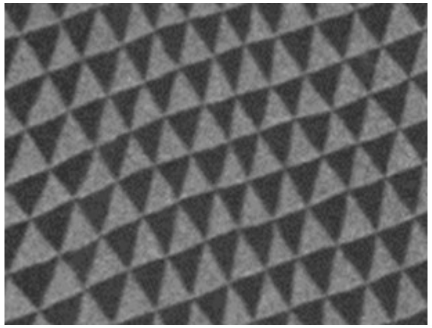

For G/hBN heterostructures, with a 1.8% lattice mismatch, requires too much hydrostatic strain to be compensated by the adhesion energy gain even inside perfect stacking domains: lattice relaxation in G/hBN can only be a weak perturbation, even for perfectly aligned heterostructures.

graphene sublattice → σ_3 ; graphene valley → τ_3

$$\hat{H} = v\boldsymbol{p}\cdot\boldsymbol{\sigma} + u_0 v b f_1(\boldsymbol{r}) + u_3 v b f_2(\boldsymbol{r})\sigma_3\tau_3 + u_1 v\left[\boldsymbol{l}_z \times \nabla f_2(\boldsymbol{r})\right]\cdot\boldsymbol{\sigma}\tau_3$$
$$+ \underline{\tilde{u}_0 v b f_2(\boldsymbol{r}) + \tilde{u}_3 v b f_1(\boldsymbol{r})\sigma_3\tau_3} + \tilde{u}_1 v\left[\boldsymbol{l}_z \times \nabla f_1(\boldsymbol{r})\right]\cdot\boldsymbol{\sigma}\tau_3$$

Weak lattice relaxation:
graphene lattice may adjust to the periodic modulation of vdW force

$$\vec{\ell}(\vec{r}) = \sum_m \vec{\ell}_m e^{i\vec{b}_m\vec{r}} \qquad u_i = u_i(d + \ell_z)$$

↓

$$f_1(\boldsymbol{r}) = \sum_{m=0\ldots5} e^{i\boldsymbol{b}_m\cdot\boldsymbol{r}}\, e^{i\vec{G}_m\vec{\ell}(\vec{r})}$$
$$f_2(\boldsymbol{r}) = i\sum_{m=0\ldots5}(-1)^m e^{i\boldsymbol{b}_m\cdot\boldsymbol{r}}\, e^{i\vec{G}_m\vec{\ell}(\vec{r})}$$

↓

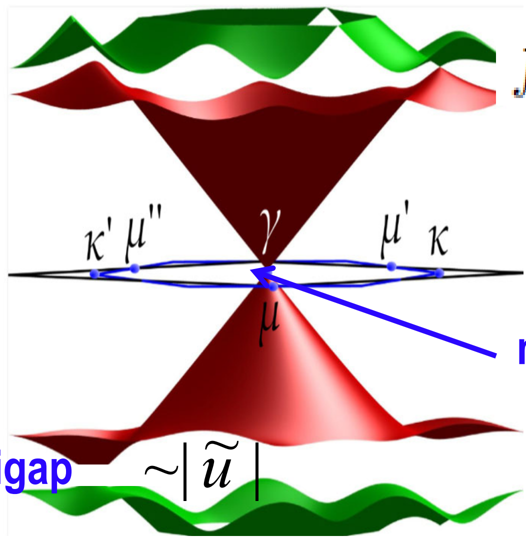

minigap at the band edge $\sim|\tilde{u}u| + |\vec{\ell}||\tilde{u}|$

minigap $\sim|\tilde{u}|$

Faraday Discussion 173 (2014); Ann. Phys. 527, 359 (2015)

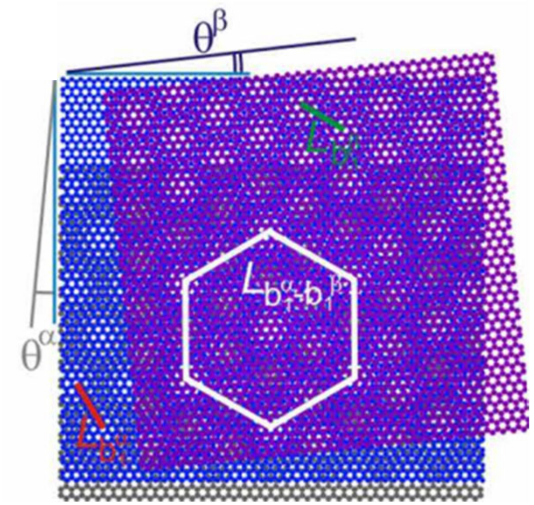

Composite 'super-moirés' in double-aligned graphene heterostructures

$$\hat{H} = v\boldsymbol{p}\bullet\boldsymbol{\sigma} + \Sigma_{j=\pm}\Sigma_{n=0\ldots5}\left[U_0^j + \left(-1\right)^n\left(\mathrm{i}U_3^j\sigma_3 + U_1^j\frac{\boldsymbol{a}_n\bullet\sigma}{a}\right)\right]\times e^{i\boldsymbol{b}_n^j\bullet\left(\boldsymbol{r}+j\frac{\boldsymbol{R}}{2}\right)}\, e^{i\boldsymbol{G}_n\bullet\boldsymbol{u}(r,\boldsymbol{R})}$$

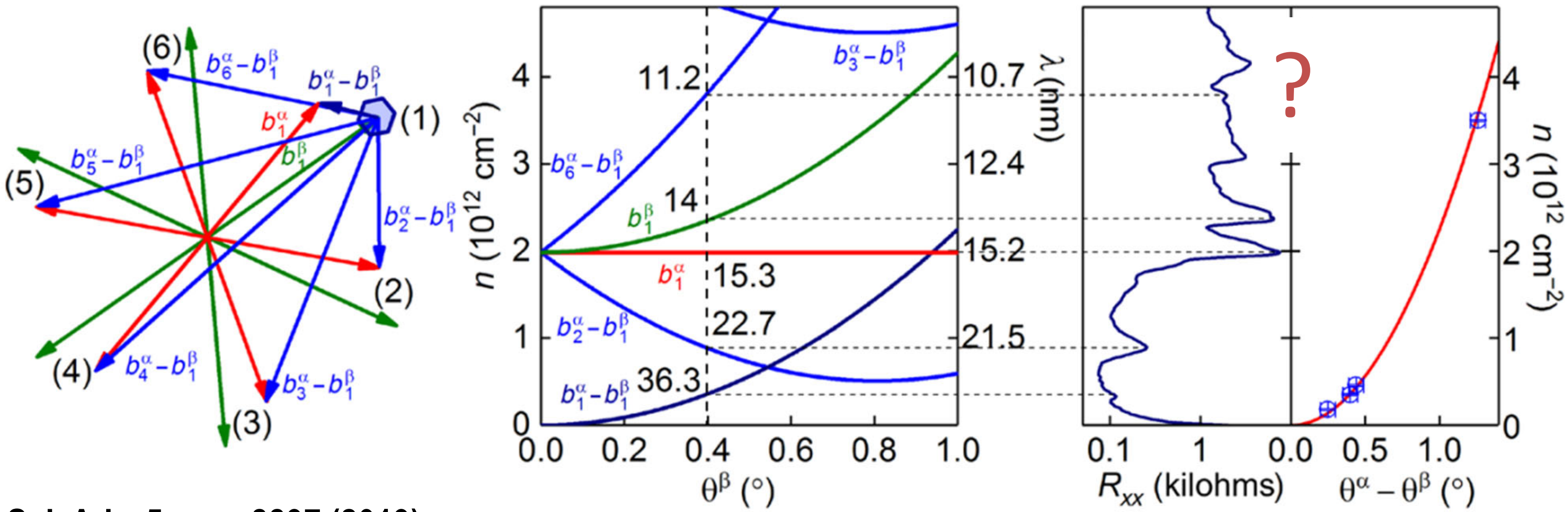

Sci. Adv. 5, eaay8897 (2019)

Graphene superlattices

- Moiré superlattice (SL) in heterostructures graphene/hexagonal boron nitride (G/hBN)
- Weak lattice relaxation in G/hBN
- Super-moiré structures
- Brown-Zak magnetic minibands ('Hofstadter butterfly') and 'kagome oscillations'
- Moiré SL effects in BLG and thin graphitic films

Brown-Zak magnetic minibands

(‘Hofstadter butterfly’)

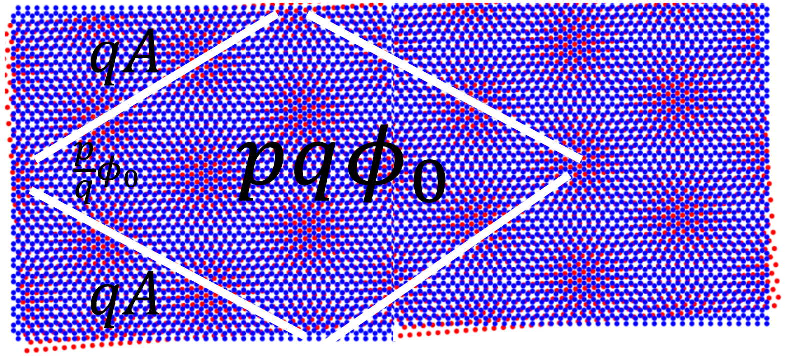

Brown - PR 133, A1038 (1964); Zak - PR 134, A1602 & A1607 (1964)

$$\phi \equiv BS = \frac{p}{q}\phi_0$$

$$G_M = \{\Theta_{\vec{X}}, \vec{X} = m_1\vec{a}_1 + m_2\vec{a}_2\} \supset G_{qM} = \{\Theta_{\vec{R}}, \vec{R} = qm_1\vec{a}_1 + qm_2\vec{a}_2\}$$

in magnetic field, group of translations is non-Abelian…

… but for rational flux values, lattice in magnetic field can be described as a ‘B=0’ superlattice with a q^2 times bigger supercell and Wannier states in a q^2 times smaller Brillouin mini-zone

Aharonov-Bohm phase

Aharonov & Bohm, PRB 115, 485 (1959)

$$\Theta_X \Theta_{X'} = e^{-i2\pi BS_{XX'}/\phi_0}\Theta_{X'}\Theta_X$$

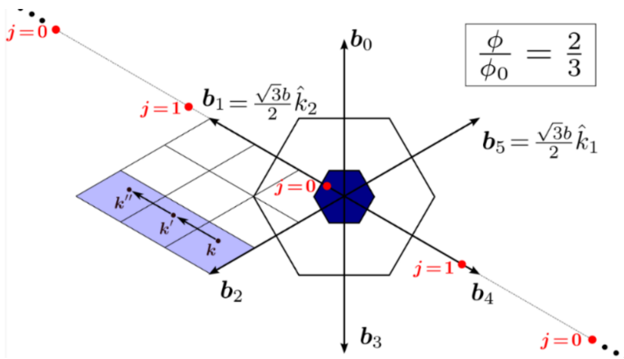

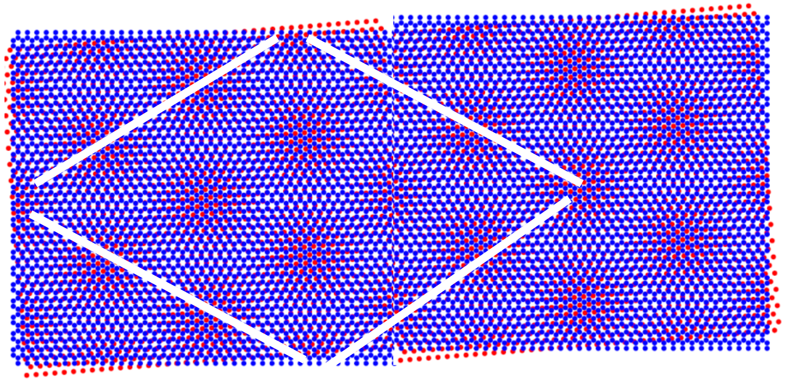

Zak-Brown magnetic minibands

Brown, PR 133, A1038 (1964); Zak, PR 134, A1602 & A1607 (1964)

$$\phi \equiv BS = \frac{p}{q}\phi_0$$

For rational values of magnetic field flux through the supercell, electrons behave as in crystals without a magnetic field, but with a q^2 times bigger supercell and q^2 times smaller Brillouin zone, where each state is q times degenerate

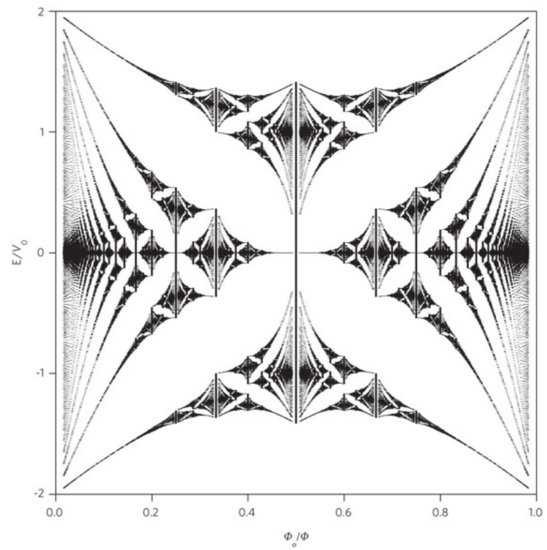

Hofstadter, PRB 14, 2239 (1976)

Brown-Zak magnetic minibands
(‘Hofstadter butterfly’)

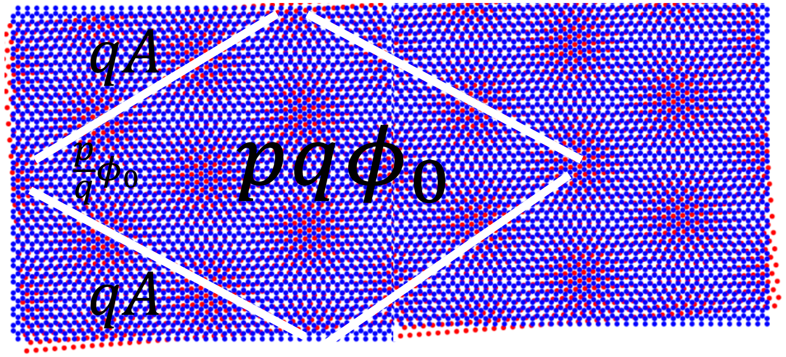

Brown - PR 133, A1038 (1964); Zak - PR 134, A1602 & A1607 (1964)

$$\phi \equiv BS = \frac{p}{q}\phi_0$$

T = 0.3 – 4 K

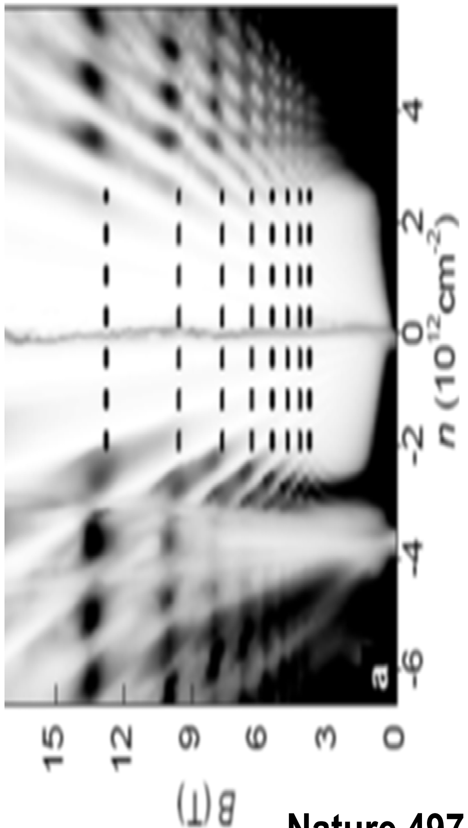

Magnetic minibands at rational values of magnetic field flux per super-cell

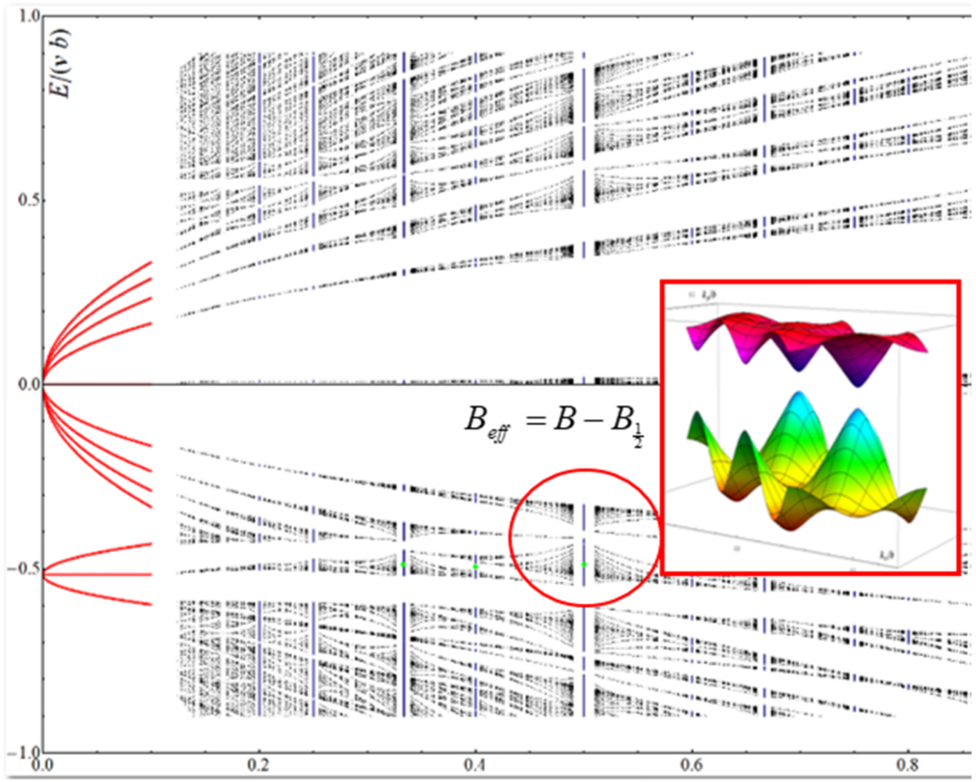

Nature 497, 594 (2013)

Phys Rev B 89, 075401 (2014)

As good bands as any: quantum Hall effect states in Landau levels spinning ofrom magnetic minibands near $\phi=\phi_0$

Nature Phys 10, 525 (2014)

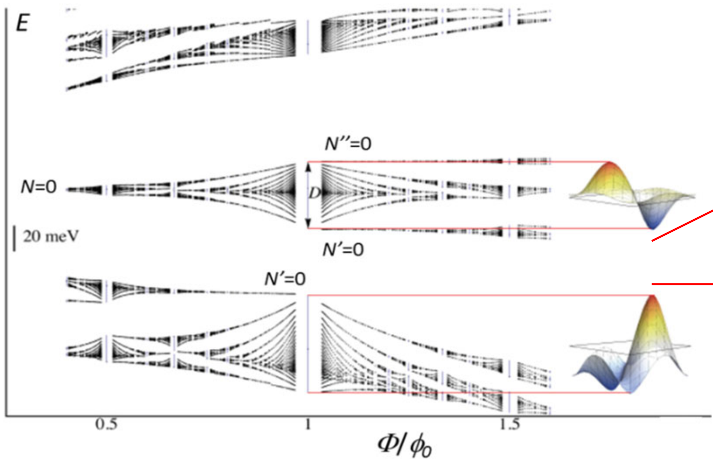

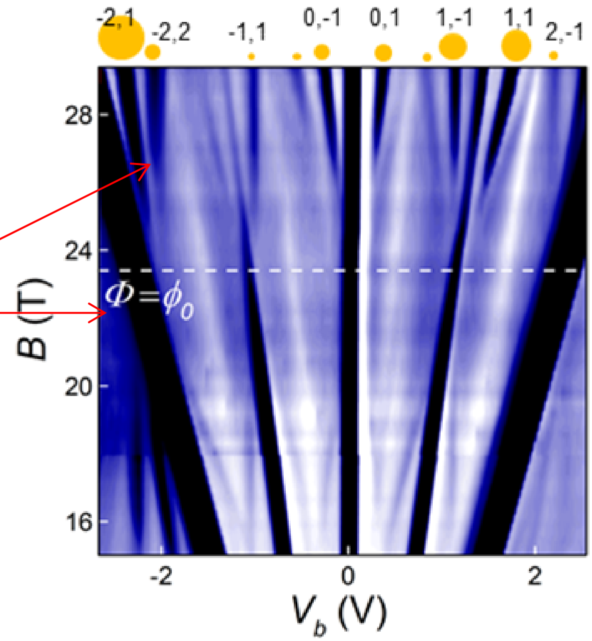

In each miniband at $\phi = \frac{p}{q}\phi_0$ electrons move with miniband dispersion as if there is no magnetic field, but slightly away from each main fraction their miniband motion happens in an effective field $B_{eff}=B-B_{p/q}$

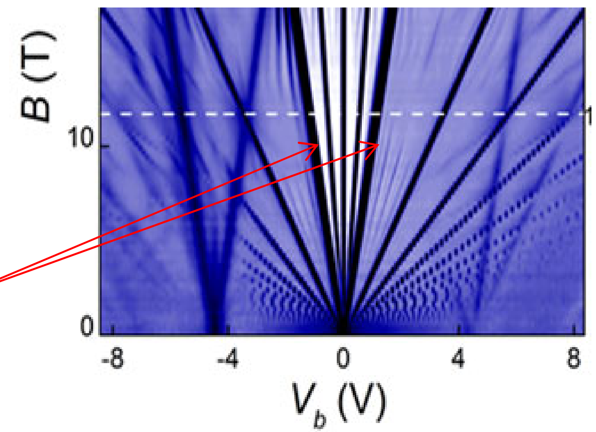

incompressible ferromagnetic quantum Hall states of primary Dirac electrons

High-temperature Brown-Zak oscillation

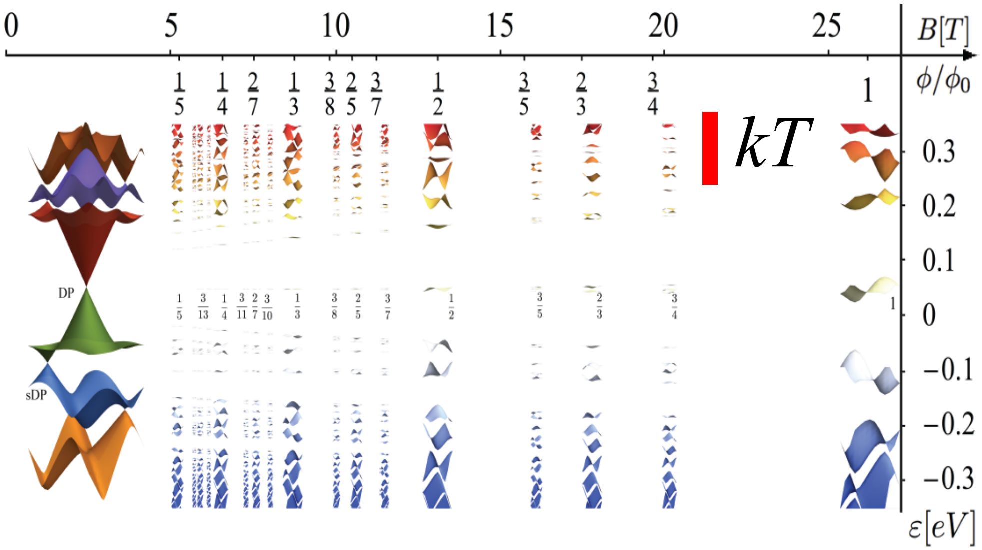

In each miniband at $\phi = \frac{p}{q}\phi_0$ electrons move with a miniband dispersion as if there is no magnetic field, but slightly away from each main fraction their miniband motion happens in an effective field

$$B_{eff}=B-B_{p/q}$$

$$\sigma_{xx}(B_{\text{eff}}) = \frac{\sigma_{xx}('0')}{1+[\omega_c(B_{\text{eff}})\tau]^2}$$

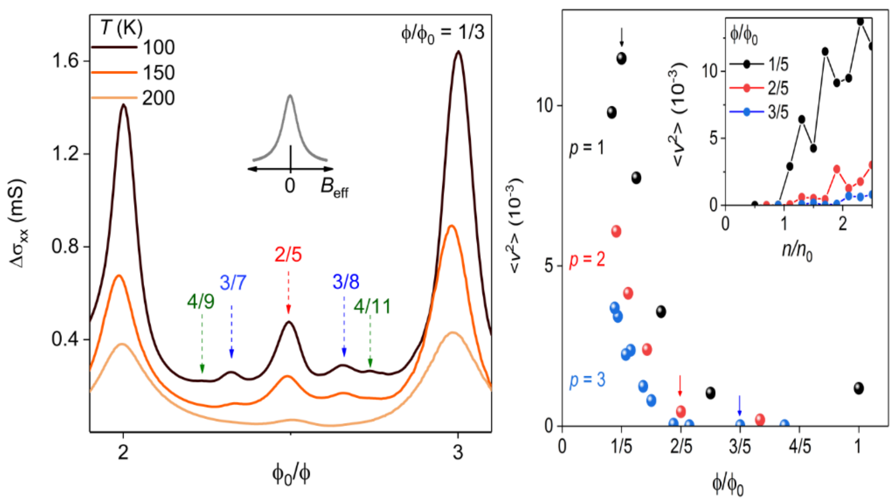

Science 357, 181 (2017); PNAS 115, 5135 (2018)

Twisted tetralayer (2+2)

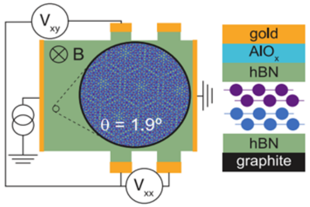

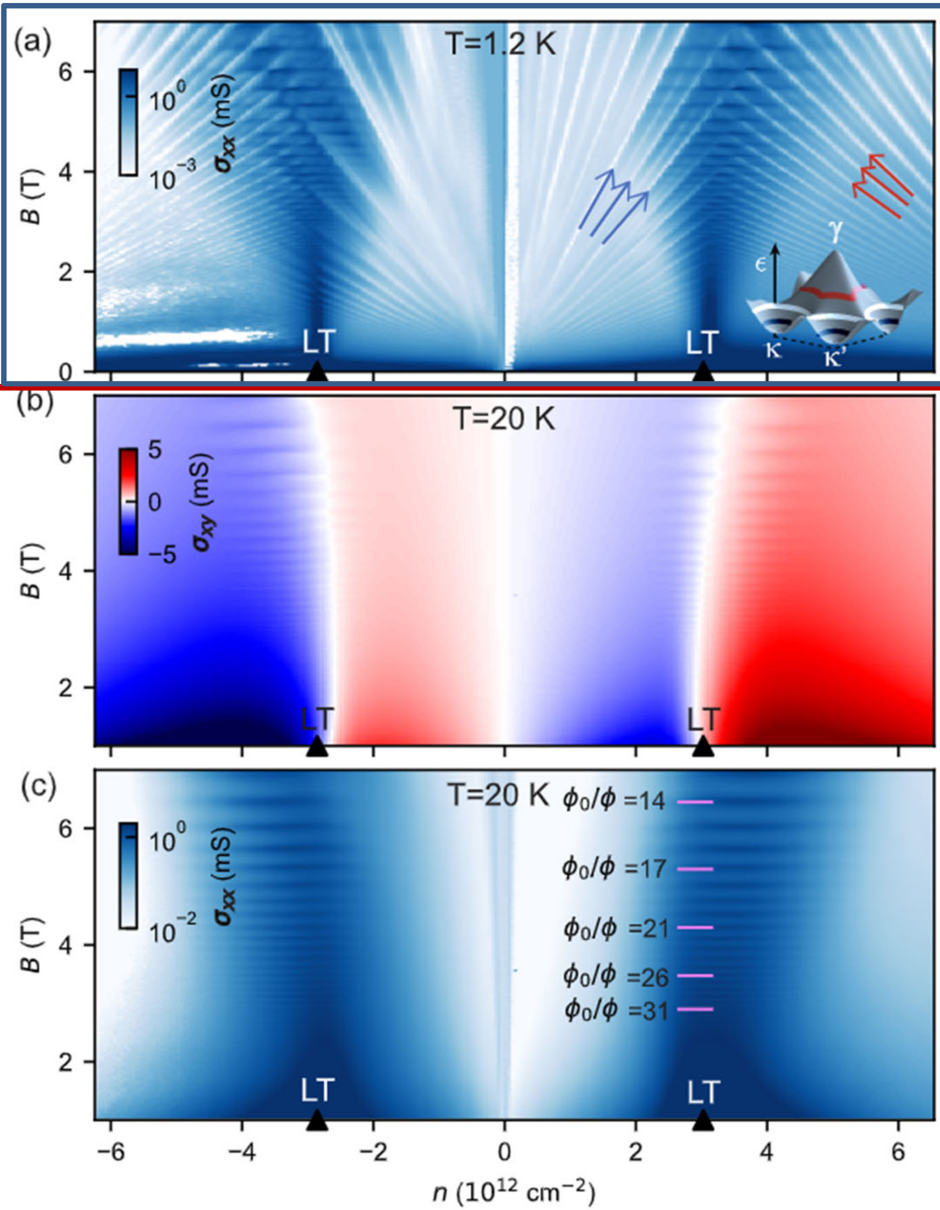

Low T: Shoubnikov – de Haas

arXiv:2303.06403

at low B, high T BZO can be traced to Lifshitz transitions in the minibands

Lifshitz transition in moiré superllatice minibands in graphene superlattices

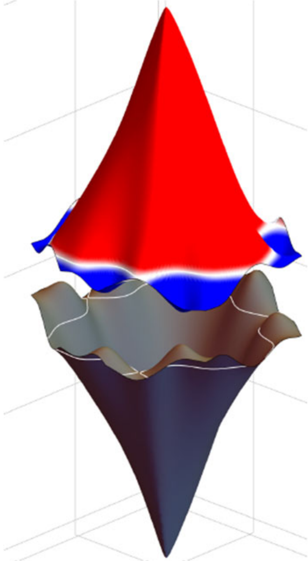

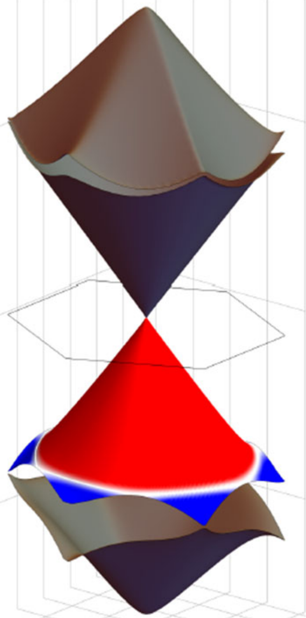

tDBLG (2+2)

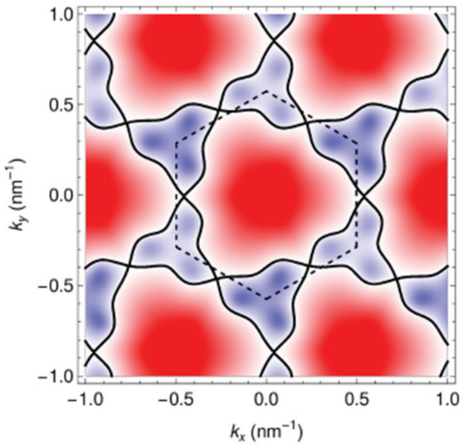

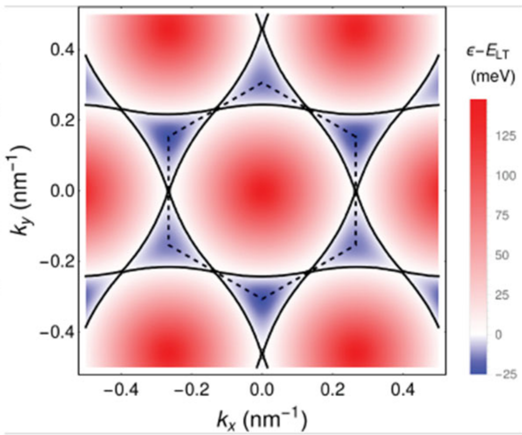

G/hBN

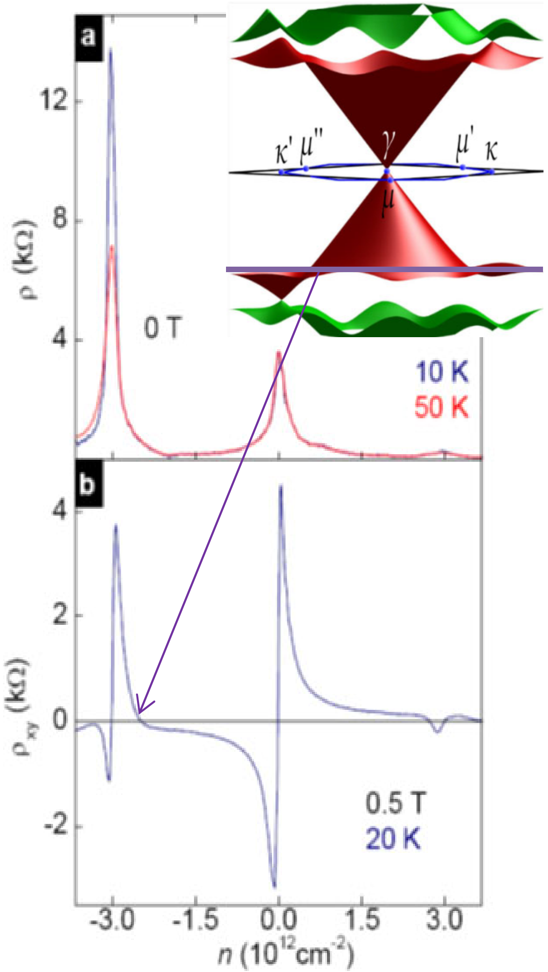

Nature 497, 594 (2013)

$$\dot{\mathbf{p}} = eB\hat{\mathbf{z}} \times \dot{\mathbf{r}}$$

$$\dot{\mathbf{r}} \equiv \mathbf{v} = \nabla_{\mathbf{p}}\epsilon(\mathbf{p})$$

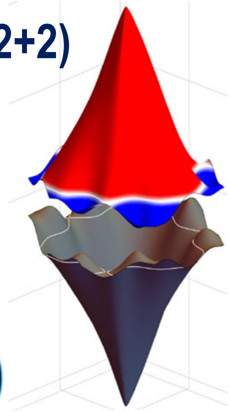

miniband Lifshitz transition

kagome-shaped network of open orbits at the Lifshitz transition

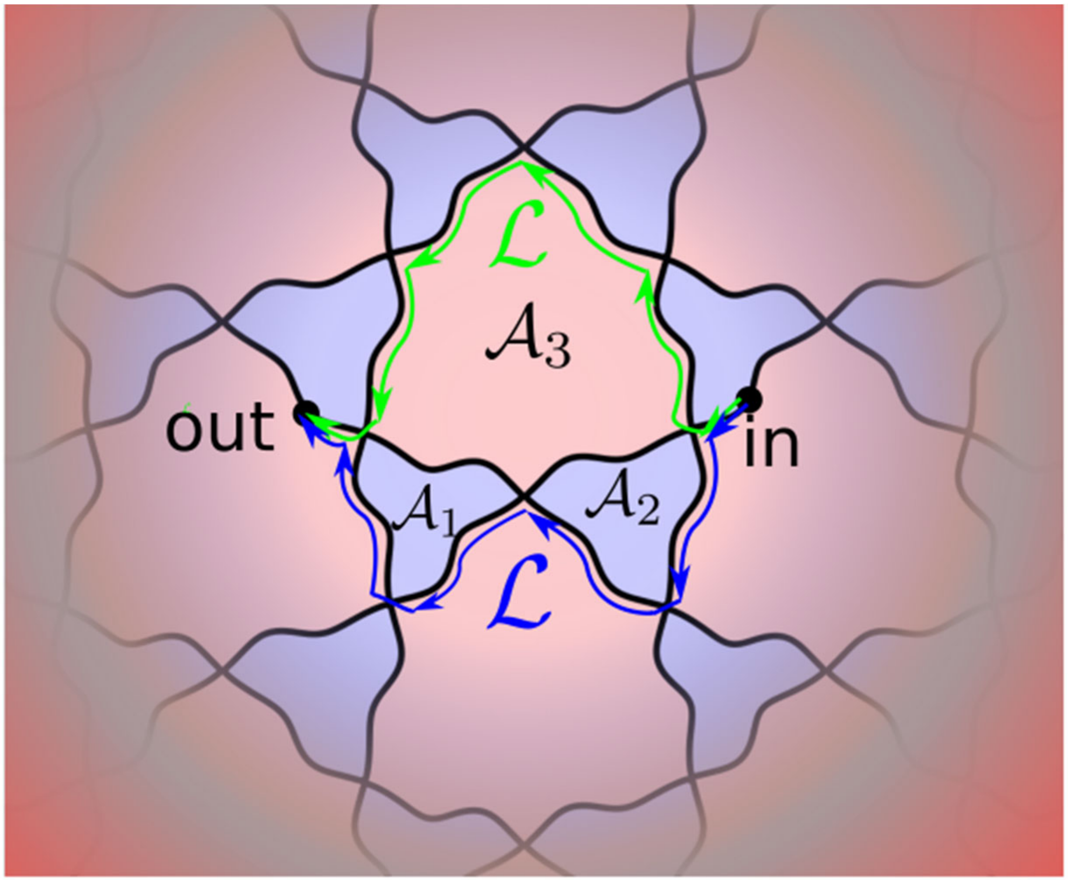

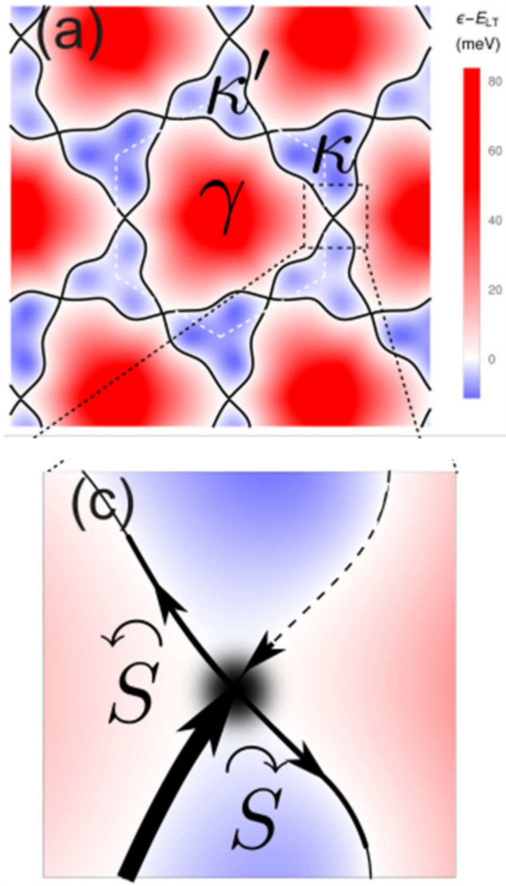

$$\frac{|\overset{\curvearrowright}{S}|}{|\overset{\curvearrowleft}{S}|} = e^{\pi\mu};\ \mu = \frac{\pi\hbar\,(\epsilon - E_{\mathrm{LT}})}{eB\mathfrak{r}}$$

$$|\overset{\curvearrowright}{S}|^2 + |\overset{\curvearrowleft}{S}|^2 = 1$$

Kagome quantum oscillations in graphene superlattices

$$\langle \mathrm{out}|\mathrm{in}\rangle = \alpha_{\mathrm{diff}} + e^{i\varphi}\left[\overset{\curvearrowleft}{S}^{3}\overset{\curvearrowright}{S}^{2} + \overset{\curvearrowleft}{S}^{3}\overset{\curvearrowright}{S}^{2} e^{i\frac{eB\mathcal{A}}{\hbar}}\right]$$

partial waves arriving along shortest ballistic paths

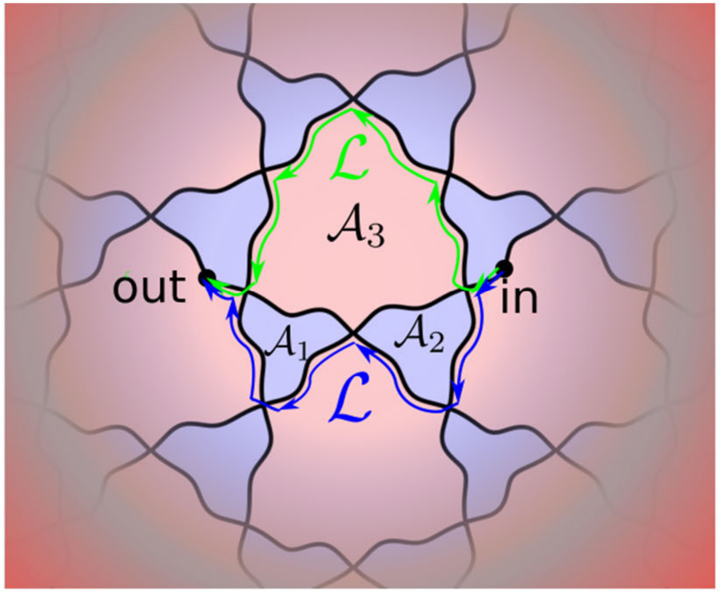

$$\mathcal{A} \equiv \mathcal{A}_1 + \mathcal{A}_2 + \mathcal{A}_3 = \frac{A_{\mathrm{BZ}}}{(eB)^2} \equiv \frac{\phi_0^2}{A_{\hexagon} B^2}$$

flux = area * *B*

$$\Delta\sigma_{\mathrm{LT}} \sim \frac{e^2}{h}\cos\frac{2\pi\phi_0}{A_{\hexagon}B} \times e^{-\frac{2\mathcal{L}}{\ell}} \int d\epsilon \, \frac{\partial n_F}{\partial\epsilon} |\overset{\curvearrowleft}{S}^{6}\overset{\curvearrowright}{S}^{4}|$$

Feature of the LT network: alternative ballistic paths are composed of segments of the same shapes and lengths, which cancels out large dynamical energy-dependent phases from the interference term (only AB phase remains):
interference correction to conductivity is not suppresses by smearing the Fermi step (in contrast to SdHO) but is sensitive to scattering

Kagome quantum oscillations in graphene superlattices

$$\langle \mathrm{out}|\mathrm{in}\rangle = \alpha_{\mathrm{diff}} + e^{i\varphi}\left[\overset{\curvearrowleft}{S}{}^{3}\,\overset{\curvearrowright}{S}{}^{2} + \overset{\curvearrowleft}{S}{}^{3}\,\overset{\curvearrowright}{S}{}^{2}\, e^{i\frac{eB\mathcal{A}}{\hbar}}\right]$$

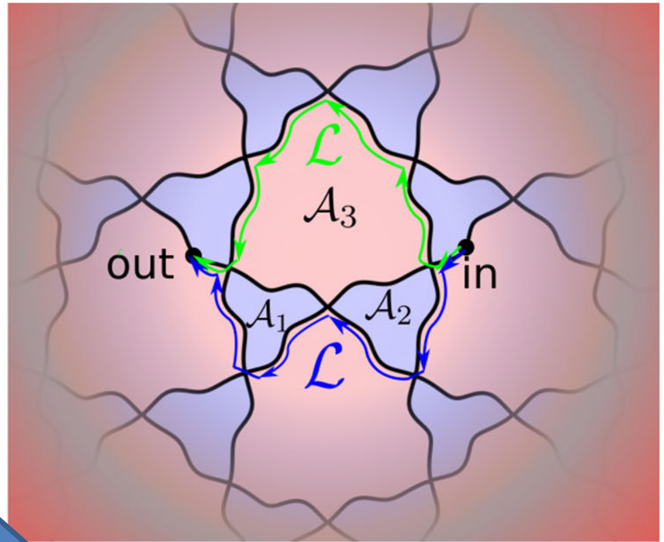

$$|\overset{\curvearrowleft}{S}|^2 + |\overset{\curvearrowright}{S}|^2 = 1 \qquad \frac{|\overset{\curvearrowright}{S}|}{|\overset{\curvearrowleft}{S}|} = e^{\pi\mu};\ \mu = \frac{\pi\hbar(\epsilon - E_{\mathrm{LT}})}{eB\mathfrak{r}}$$

$$\Delta\sigma_{\mathrm{LT}} \sim \frac{e^2}{h}\cos\frac{2\pi\phi_0}{\mathcal{A}_{\hexagon}B} \times e^{-\frac{2\mathcal{L}}{\ell}} \int d\epsilon\, \frac{\partial n_F}{\partial\epsilon} |\overset{\curvearrowleft}{S}{}^{6}\,\overset{\curvearrowright}{S}{}^{4}|$$

$$\sim e^{-\frac{(n-n_{\mathrm{max}})^2}{\delta n^2}}\, e^{-\frac{2\mathcal{L}(B)}{\ell(T)}}\, \cos\frac{2\pi\phi_0}{\mathcal{A}_{\hexagon}B}$$

$$n_{\mathrm{max}} = n_{\mathrm{LT}} \pm \frac{2\rho B\mathfrak{r}}{5\phi_0}$$

± depends only on whether ‘hexagonal’ area hosts hole-like (+) or electron-like (-) branch

Kagome quantum oscillations in graphene superlattices

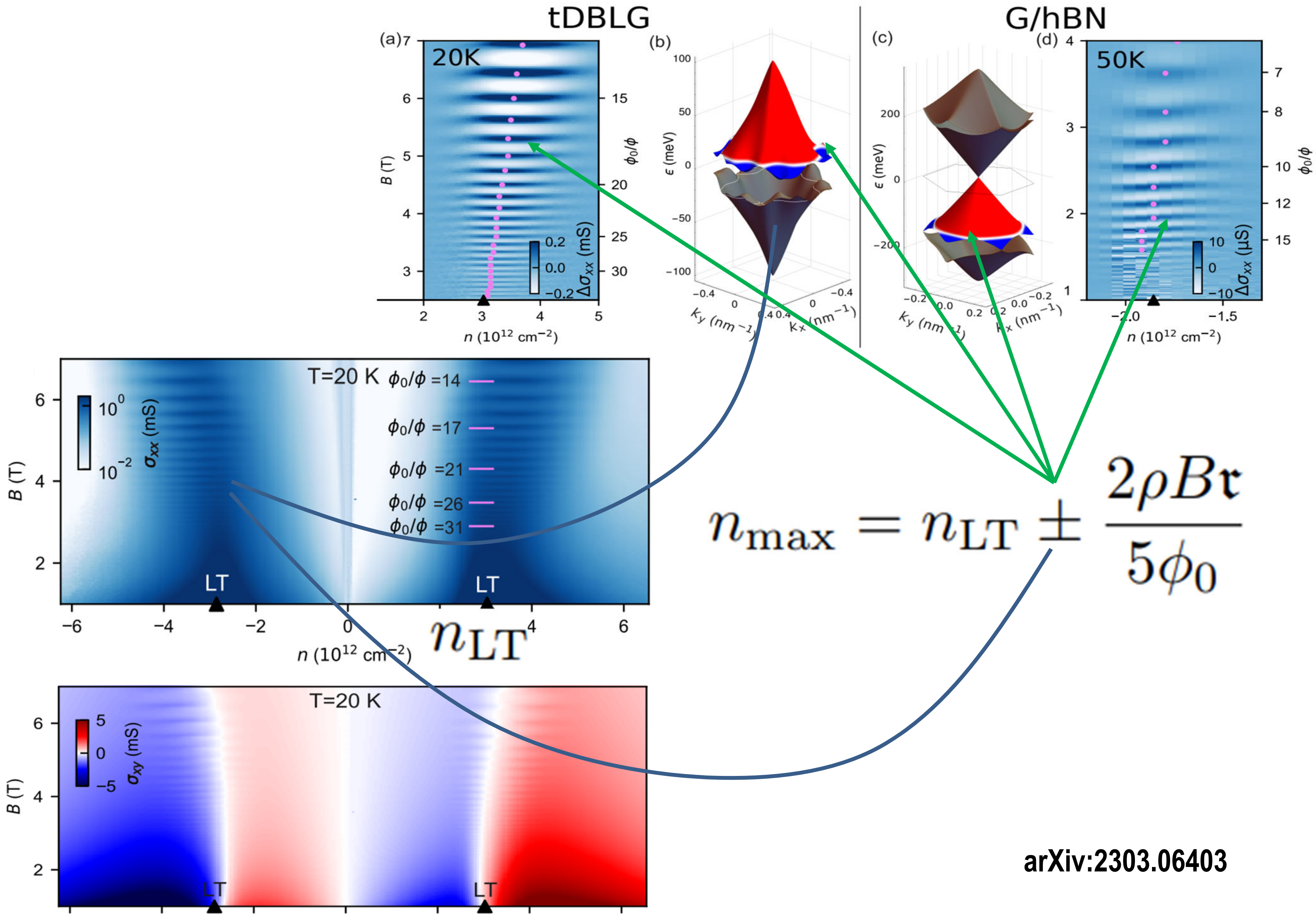

$$n_{\max} = n_{\mathrm{LT}} \pm \frac{2\rho B \mathfrak{r}}{5\phi_0}$$

arXiv:2303.06403

Graphene superlattices

- Moiré superlattice (SL) in heterostructures graphene/hexagonal boron nitride (G/hBN)
- Weak lattice relaxation in G/hBN
- Super-moiré structures
- Brown-Zak magnetic minibands ('Hofstadter butterfly') and 'kagome oscillations'
- Moiré SL effects in BLG and thin graphitic films

Moiré and Brown-Zak minibands in bilayer graphene (BLG) aligned with hBN

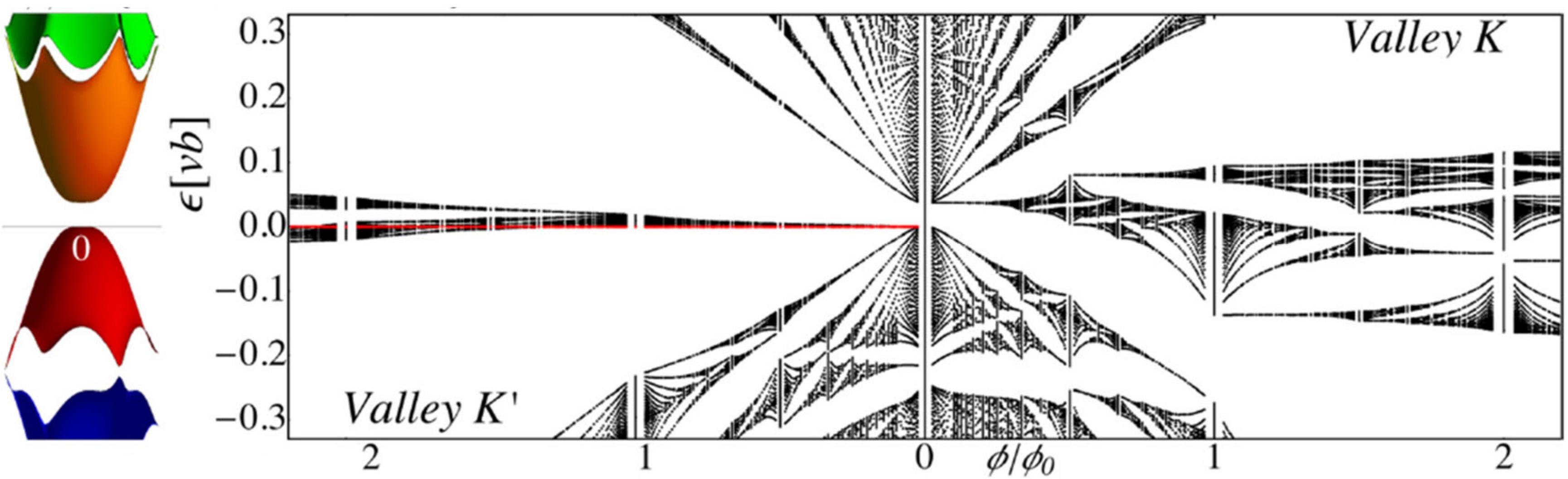

- G/hBN moiré interface breaks inversion symmetry of BLG (interlayer asymmetry gap)
- In BLG, zero-energy Landau levels for K and –K valleys reside in different layers

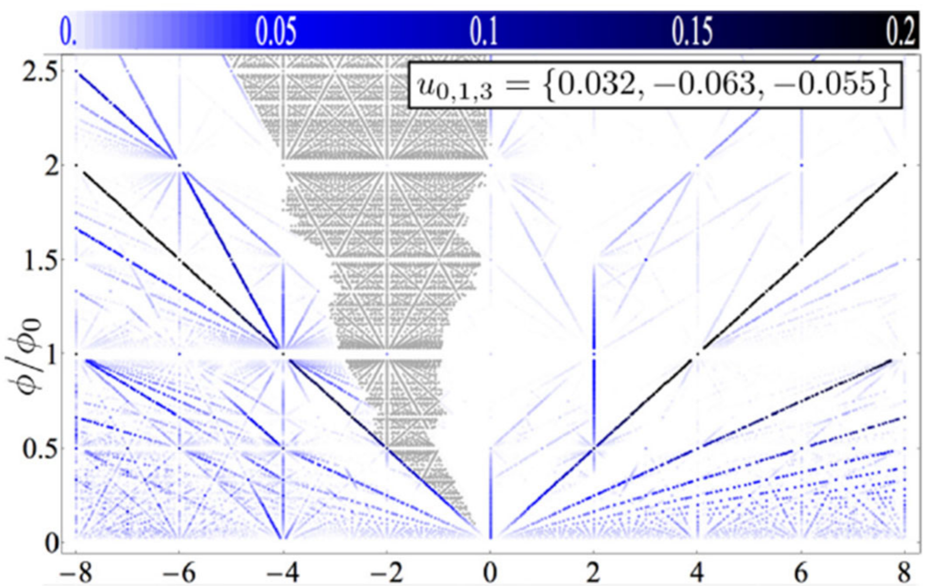

Phys Rev B 94, 045442 (2016)

Electrostatically induced surface states in graphite and minibands due to surface moiré pattern

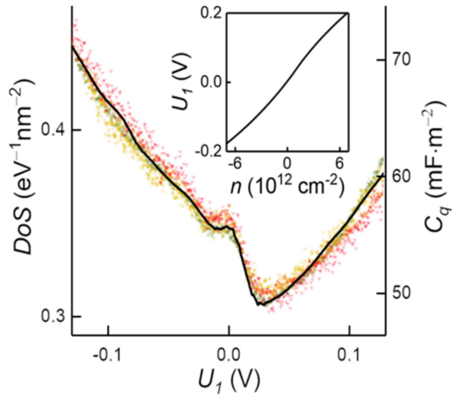

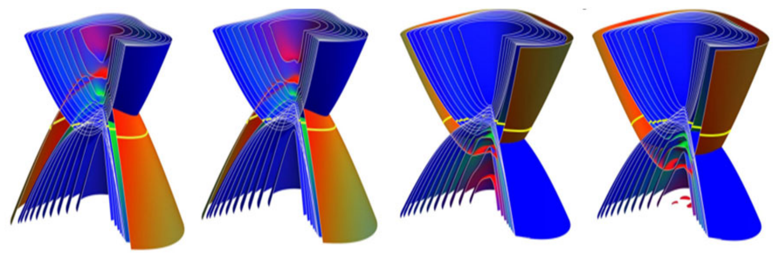

electrostatically controlled surface states in graphite, located at 2-3 surface monolayers

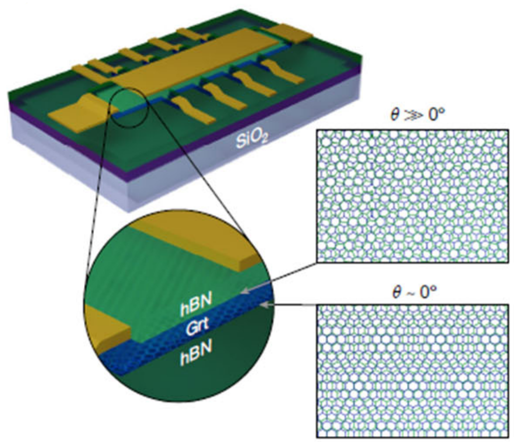

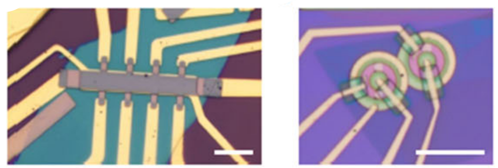

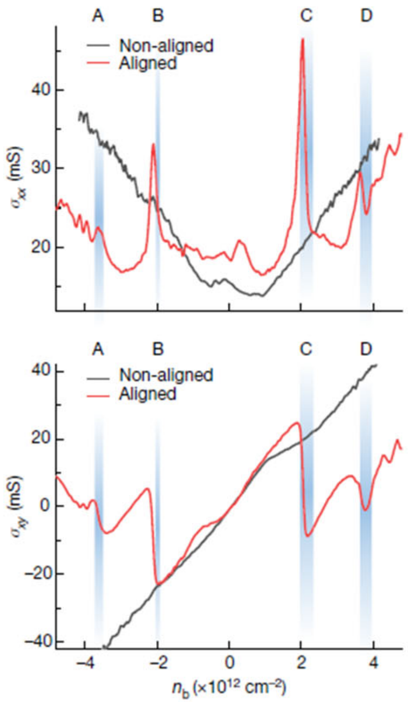

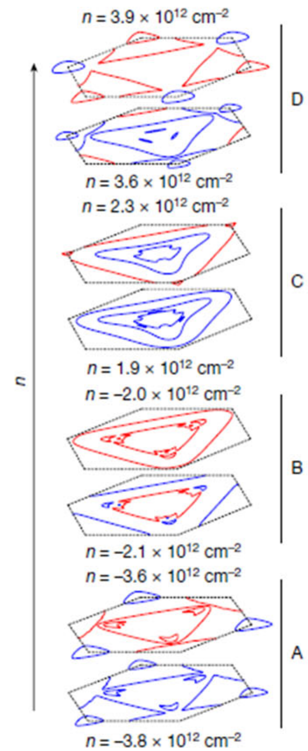

Nature 620, 756 (2023)

Brown-Zak ‘kagome’ oscillations in graphite/hBN superlattices due to surface states

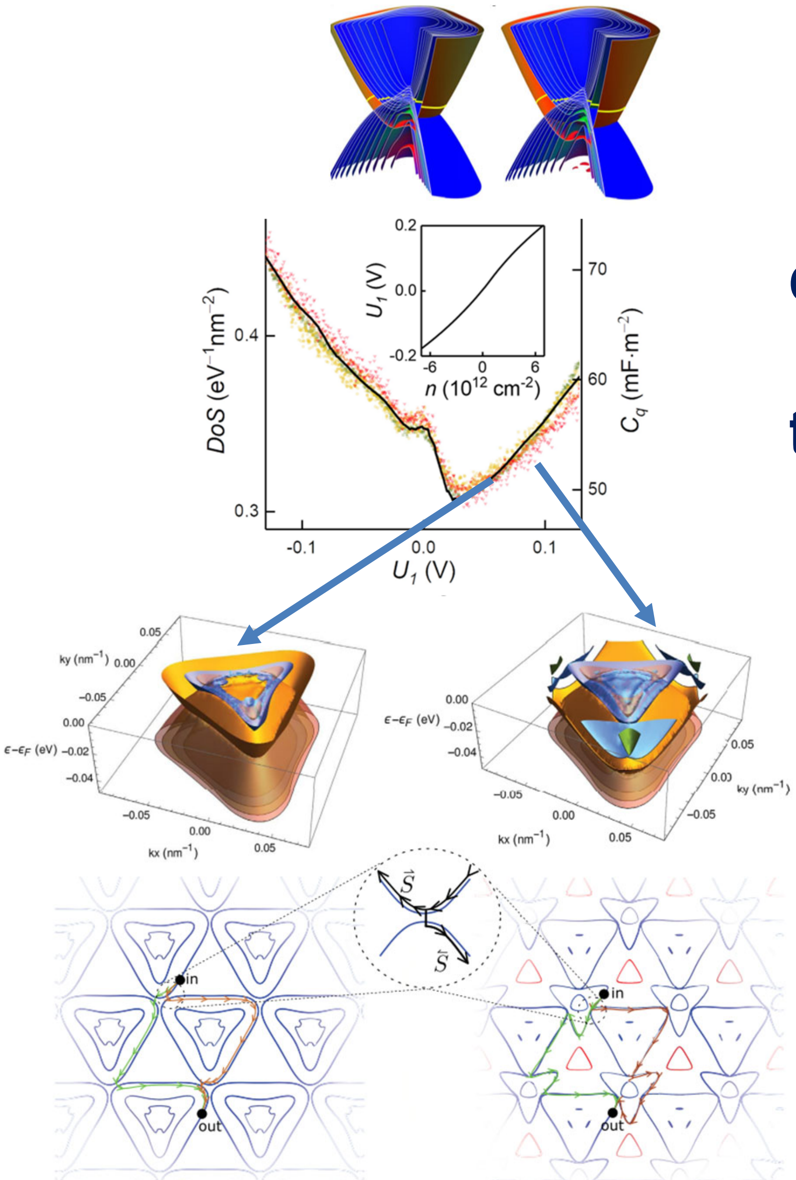

electrostatically controlled by the closest gate

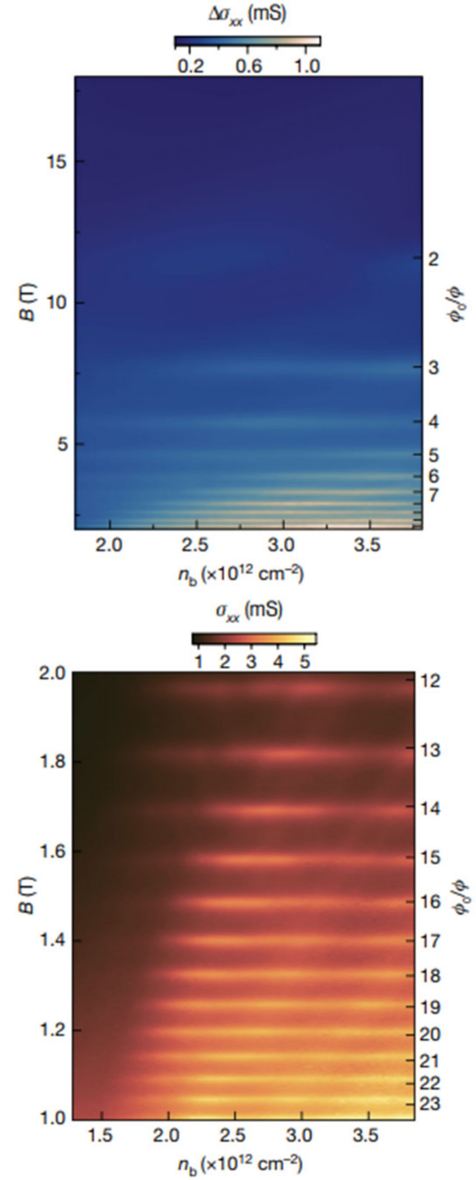

Nature 620, 756 (2023)

Brown-Zak oscillations in graphite/hBN superlattices due to bulk states (caused by tails of strain on the surface?)

$n_t=n_b$ $B>5.5T$

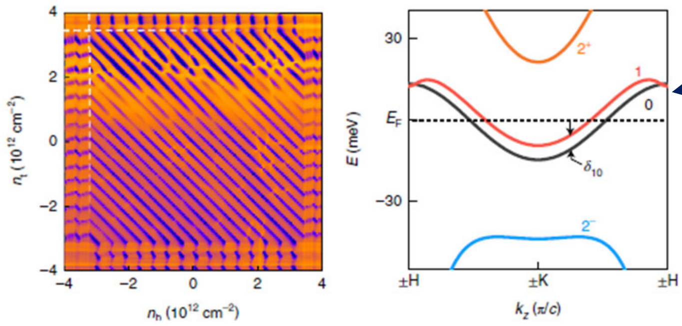

Bands coming from K valley ‘zero-energy’ Landau levels that reside on even layers and –K valley on odd layers

Nature Physics 15, 437 (2019)

Nature 620, 756 (2023)

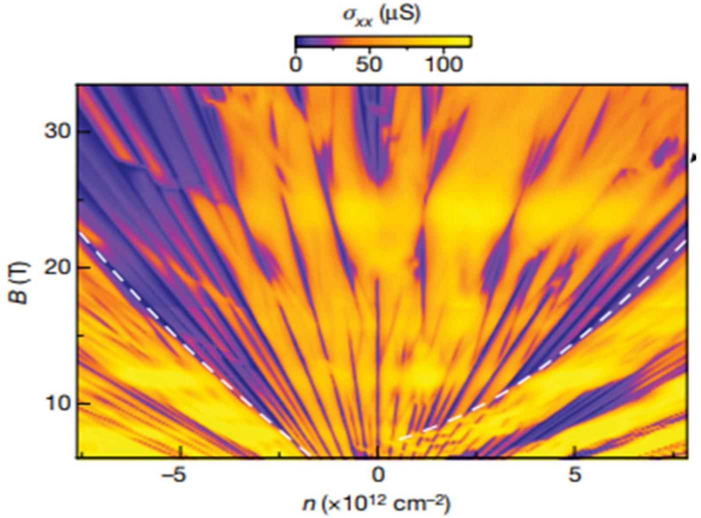

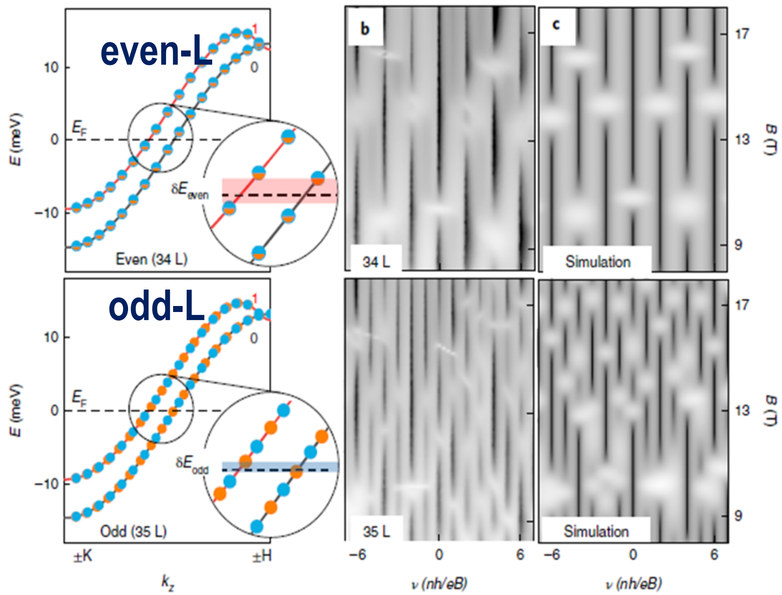

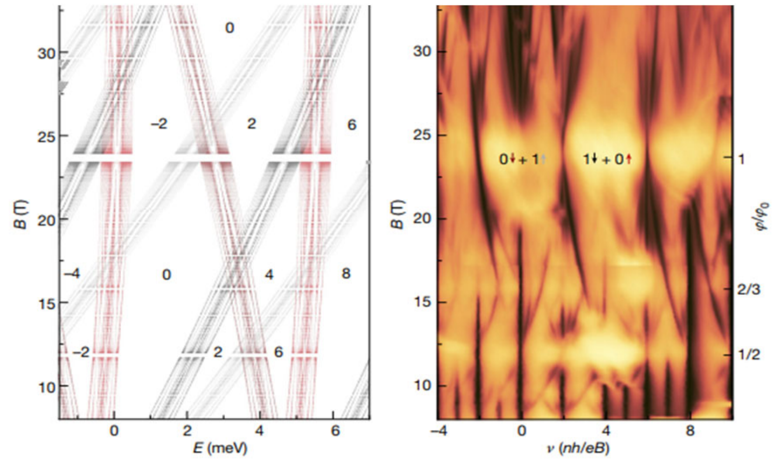

Graphene superlattices

Sergey Slizovskiy
Xi Chen
John Wallbank
Aavishkar Patel
Ed McCann

Andre Geim (NGI)
Artem Mishchenko (NGI)
David Goldhaber-Gordon (Stanford)
Klaus Ensslin (ETH)
Thomas Ihn (ETH)
Roshan Kumar (ICFO)
Kostya Novoselov (NUS)